

Latent Space Smoothing for Individually Fair Representations

Momchil Peychev, Anian Ruoss, Mislav Balunović, Maximilian Baader, Martin Vechev
 Department of Computer Science, ETH Zurich

{momchil.peychev, anian.ruoss, mislav.balunovic, mbaader, martin.vechev}@inf.ethz.ch

Abstract

Fair representation learning encodes user data to ensure fairness and utility, regardless of the downstream application. However, learning individually fair representations, i.e., guaranteeing that similar individuals are treated similarly, remains challenging in high-dimensional settings such as computer vision. In this work, we introduce LASSI, the first representation learning method for certifying individual fairness of high-dimensional data. Our key insight is to leverage recent advances in generative modeling to capture the set of similar individuals in the generative latent space. This allows learning individually fair representations where similar individuals are mapped close together, by using adversarial training to minimize the distance between their representations. Finally, we employ randomized smoothing to provably map similar individuals close together, in turn ensuring that local robustness verification of the downstream application results in end-to-end fairness certification. Our experimental evaluation on challenging real-world image data demonstrates that our method increases certified individual fairness by up to 60%, without significantly affecting task utility.

1. Introduction

Deep learning models are increasingly being deployed in important domains such as credit scoring [39], crime risk assessment [6], face detection [71], and others where decisions of the model can have significant impact on the society. Unfortunately, both models and datasets employed in these settings were shown to be biased [7, 44] which raised concerns of their usage in such tasks, and caused regulators to hold organizations accountable for the discriminatory effects of their models [20, 21, 23, 24, 74].

Fair representation learning [84] is a promising bias mitigation approach that transforms data to prevent discrimination regardless of the downstream application, while maintaining high task utility. The approach is highly modular [57], with a *data regulator* defining the fairness notion, a *data producer* learning the fair representation, and *data*

consumers employing the transformed data in downstream tasks. However, although recent work successfully learned representations with fairness guarantees [25, 65], the application to high-dimensional data, such as images, remains challenging.

Key challenge: scaling to high-dimensional data and real-world models The two central challenges in *individually* fair representation learning are: (i) designing a suitable input similarity metric [82, 84], and (ii) enforcing that similar individuals are provably treated similarly (according to the designed metric). For low-dimensional tabular data, prior work typically measures input similarity in terms of input features (age, income, *etc.*), using, *e.g.*, logical constraints [65] or weighted ℓ_p -metrics [81]. However, fairness issues have also been observed in widely used settings with high-dimensional data such as facial analysis [7]. The key issue is that characterizing the similarity of images at the input-level (as done in prior work [65]), *e.g.*, by comparing pixels, is impractical. Moreover, proving that all points in the infinite set of similar individuals receive the same outcome entails propagating this set through the model, which is out of reach for prior approaches that rely on (mixed-integer) linear programming solvers [18, 73] and only scale to small networks, not useful for high-dimensional data.

This work In this work, we introduce Latent Space Smoothing for Individually fair representations (LASSI), a method which addresses both of these challenges. Our approach is enabled by two recent advances: emerging of powerful generative models [42], which allow defining individual fairness for images, and scalable certification of deep models [11], which allows proving individual fairness. A high-level overview of our approach is shown in Fig. 1. Concretely, we use generative modeling [42] to enable data regulators to define input similarity by varying some continuous attribute of the image, such as pale skin in Fig. 1. To enforce that similar individuals are provably treated similarly, we base our approach on smoothing: (i) the data producer uses center smoothing [45] in order to learn a representation that provably maps similar individuals close together,

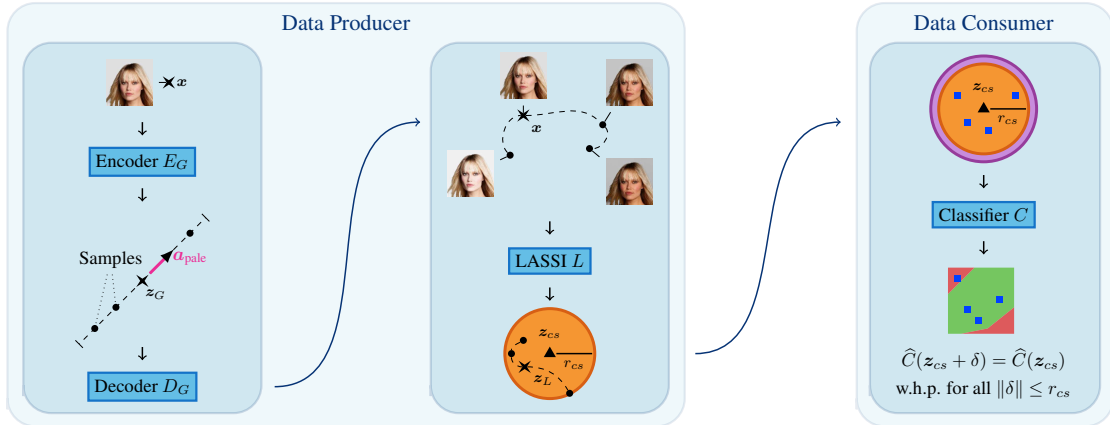


Figure 1. Overview of LASSI. The left part shows the data producer who captures the set of individuals similar to x by interpolating along the attribute vector \mathbf{a}_{pale} . The data producer then uses adversarial training [54] and center smoothing [45] to compute a representation that provably maps all similar points into the ℓ_2 -ball of radius r_{cs} around z_{cs} . The right part shows the data consumer who can then certify individual fairness, *i.e.*, prove that all similar individuals receive the same classification outcome, of the end-to-end model by checking whether the certified radius obtained via randomized smoothing [11] exceeds r_{cs} .

and (ii) the data consumer certifies local ℓ_2 -robustness using randomized smoothing [11], thereby proving individual fairness of the end-to-end model.

To measure input similarity, the data producer leverages the ability of a bijective generative model to interpolate in the latent space along the direction of the attribute vector. Consequently, the set of similar individuals is given by a line segment (lower left of Fig. 1), corresponding via the bijection to an elaborate curve in the input space (top middle of Fig. 1). However, this curve in the input space cannot be easily captured by an ℓ_p -ball. Therefore, the data producer learns a representation $L \circ D_G$ that maps all points of the latent line segment close together by using adversarial training to minimize the distance between similar individuals. As adversarial training does not provide guarantees on the maximum distance, the data producer uses center smoothing [45] to adjust the representation such that the *smoothed* encoder $\widehat{L} \circ \widehat{D}_G$ provably maps all similar points into an ℓ_2 -ball of radius r_{cs} around a center z_{cs} with high probability (lower middle of Fig. 1). Finally, the data consumer only needs to prove that the certified radius (violet, top right in Fig. 1) of its *smoothed* classifier \widehat{C} around z_{cs} is larger than r_{cs} to obtain an individual fairness certificate for the end-to-end model $\widehat{C} \circ (\widehat{L} \circ \widehat{D}_G) \circ E_G$. In this work, we always use $\widehat{\cdot}$ notation when referring to smoothed models.

Our experimental evaluation on several image classification tasks shows that training with LASSI significantly increases the number of individuals for which we can certify individual fairness by up to 60% compared to the baselines. Furthermore, we show that LASSI can increase fairness for several different sensitive attributes, as well as their combinations. We also use a procedurally generated dataset to confirm that the certificates obtained using the generative

model are sound and transfer to the ground truth dataset.

Main contributions Our main contributions are:

- A novel input similarity metric for high-dimensional data via latent space interpolation.
- A scalable representation learning method with individual fairness certification for models operating on high-dimensional data via randomized smoothing.
- An efficient implementation and an evaluation of our method on a variety of image classification tasks.

2. Related work

In this work, we consider individual fairness, which requires that similar individuals are treated similarly [16]. In contrast, group fairness enforces that specific classification statistics are equal across different groups of the population [16, 29]. While both fairness notions are desirable, they also both suffer from certain shortcomings. For instance, models satisfying group fairness may still discriminate against individuals [16] or subgroups [37]. In contrast, the central challenge limiting practical adoption of individual fairness is the lack of a widely accepted similarity metric [82]. While recent work has made progress in developing similarity metrics for tabular data [33, 55, 59, 76, 83], defining a concise similarity for high-dimensional data remains challenging and is a key goal of our work.

Fair representation learning A wide range of methods have been proposed to learn fair representations of user data. Most of these works consider group fairness and employ

techniques such as adversarial learning [17, 38, 49, 53], disentanglement [12, 51, 66], duality [70], low-rank matrix factorization [60], and distribution alignment [3, 52, 85]. Individually fair representation learning has recently gained attention, with similarity metrics based on logical formulas [65], Wasserstein distance [22, 46], fairness graphs [47], and weighted ℓ_p -norms [84]. Unfortunately, these approaches cannot capture similarity between individuals for the high-dimensional data we consider in our work.

Bias in high-dimensional data A long line of work has investigated the biases of models operating on high-dimensional data, such as images [78, 79] and text [5, 48, 61, 72], showing, *e.g.*, that black women obtain lower accuracy in commercial face classification [7, 44, 63]. Importantly, these models not only learn but also amplify the biases of the training data [31, 86], even for balanced datasets [77]. A key challenge for investigating and mitigating bias in high-dimensional data is that, unlike tabular data, sensitive attributes such as gender or skin color are not directly encoded as features. Thus, prior work often relies on generative models [2, 13, 15, 35, 40, 41, 64, 67] or computer simulations [56] to manipulate data attributes and check whether the perturbed instances are classified the same. However, unlike our work, these methods only empirically test for bias and do not provide certification guarantees. Some works also explored using generative models to define [28, 80] or certify [58] robustness, but they have not focused on fairness.

Fairness certification Regulatory agencies are increasingly holding organizations accountable for the discriminatory effects of their machine learning models [20, 21, 23, 24, 74]. Accordingly, designing algorithms with fairness guarantees has become an active area of research [1, 3, 4, 9, 25, 68]. However, unlike our work, most approaches for individual fairness certification consider pretrained models and thus cannot be employed in fair representation learning [34, 75, 81]. In contrast, Ruoss et al. [65] learn individually fair representations with provable guarantees for low-dimensional tabular data, providing a basis for our approach. However, neither the similarity notions nor the certification methods employed by Ruoss et al. [65] scale to the high-dimensional data, which is the primary focus of our work.

3. Background

This section provides background on fair representation learning, generative modelling, and randomized smoothing.

LCIFR The LCIFR framework [65] learns representations with individual fairness guarantees for low-dimensional tabular data, ensuring that for a point $\mathbf{x} \in \mathbb{R}^n$

all similar individuals are treated similarly. To achieve this, Ruoss et al. [65] define a family of similarity notions and leverage (mixed-integer) linear programming methods to propagate all similar individuals through the model. Then, if all the points satisfying the given similarity notion obtain the same classification, LCIFR has provably shown that individual fairness is satisfied at \mathbf{x} . However, high-dimensional applications remain out of reach for LCIFR because both the similarity notions and linear programming methods are customized to low-dimensional tabular data. Similarity is defined via logical formulas operating on the features of \mathbf{x} , which is infeasible for *e.g.*, images, which cannot be compared solely at the pixel level. Moreover, while the linear programming employed by Ruoss et al. [65] is known to work well for small neural networks, it does not scale to real-world computer vision models. In this work, we thus demonstrate how to resolve these two key concerns to generalize the high-level idea of LCIFR to real-world, high-dimensional applications.

Glow Normalizing flows, such as Glow [42], recently emerged as a promising approach for generative modeling due to their exact log-likelihood evaluation, efficient inference and synthesis, and useful latent space for downstream tasks. Unlike GANs [27] or VAEs [43], normalizing flows are bijective models consisting of an encoder $E_G : \mathbb{R}^n \rightarrow \mathbb{R}^q$ and a decoder $D_G : \mathbb{R}^q \rightarrow \mathbb{R}^n$ for which $\mathbf{x} = D_G(E_G(\mathbf{x}))$. The latent space of Glow captures important attributes of the data, which enables latent space interpolation such as, *e.g.*, manipulating the skin color of a person in an image. While attribute manipulation via latent space interpolation has also been investigated in the fairness context for GANs and VAEs [2, 15, 35, 40, 64], the key advantage of Glow is the existence of an encoder (unlike GANs, which cannot represent an input point in the latent space efficiently) and the bijectivity of the end-to-end model (VAEs cannot reconstruct the input point exactly). Our key idea is to leverage Glow to define the similarity between two images by interpolating along the directions defined by certain sensitive attributes in the latent space.

Randomized smoothing Recent work [11] uses randomized smoothing to provide local robustness guarantees for a given classifier $f : \mathbb{R}^k \rightarrow \mathcal{Y}$. They construct a smoothed classifier \hat{f} , which returns the most probable class under f of the input \mathbf{x} when perturbed by some $\epsilon \sim \mathcal{N}(0, \sigma^2 I)$:

$$\hat{f}(\mathbf{x}) := \arg \max_{c \in \mathcal{Y}} \mathbb{P}_{\epsilon \sim \mathcal{N}(0, \sigma^2 I)}(f(\mathbf{x} + \epsilon) = c). \quad (1)$$

The robustness certificate states that \hat{f} classifies all $\mathbf{x} + \delta$ the same as \mathbf{x} for all $\|\delta\|_2 < R$ and is given by the following:

Theorem 3.1 (from [11]). Suppose $c_A = \hat{f}(\mathbf{x}) \in \mathcal{Y}$ and $\underline{p}_A, \overline{p}_B \in [0, 1]$. If

$$\mathbb{P}_\epsilon(f(\mathbf{x}+\epsilon) = c_A) \geq \underline{p}_A \geq \overline{p}_B \geq \max_{c_B \neq c_A} \mathbb{P}_\epsilon(f(\mathbf{x}+\epsilon) = c_B),$$

then $\hat{f}(\mathbf{x} + \delta) = c_A$ for all δ satisfying $\|\delta\|_2 < R$ with $R := \frac{\sigma}{2}(\Phi^{-1}(\underline{p}_A) - \Phi^{-1}(\overline{p}_B))$.

Calculating the above quantities is typically infeasible in cases where f is a large neural network. Hence, the quantities c_A and $\mathbb{P}_\epsilon(f(\mathbf{x} + \epsilon) = c_A)$ are estimated via sampling, resulting in a (probabilistic) $1 - \alpha_s$ confidence lower bound \underline{p}_A . Thus, the certificate holds with confidence $1 - \alpha_s$. Later, for certifying classification, we will denote the standard deviation σ by σ_{cls} .

Recently, Kumar and Goldstein [45] extended this method from classification to multidimensional regression. This is particularly useful in our setting for certifying the smoothed version \hat{g} of an encoder network g , mapping to \mathbb{R}^k . As before, we rely again on sampling and approximation to evaluate \hat{g} . Specifically, $\hat{g}(\mathbf{x})$ evaluates to the center \mathbf{z}_{cs} of a minimum enclosing ball containing at least half the points in $Z = \{\mathbf{z}_i\}_{i=1}^m$ where $\mathbf{z}_i \sim g(\mathbf{x} + \mathcal{N}(0, \sigma^2 I))$. The robustness certificate results from the following theorem:

Theorem 3.2 (adapted from [45]). With probability at least $1 - \alpha_c$ we have,

$$\forall \mathbf{x}' \text{ s.t. } \|\mathbf{x} - \mathbf{x}'\|_2 \leq \epsilon, \|\hat{g}(\mathbf{x}) - \hat{g}(\mathbf{x}')\|_2 \leq r_{cs}. \quad (2)$$

Here, r_{cs} depends on the given ϵ , α_c and on a quantile of the distances $\|\hat{g}(\mathbf{x}) - g(\mathbf{z}_i)\|_2$, $\mathbf{z}_i \in Z$. We will later denote the standard deviation σ for smoothing the encoder by σ_{enc} .

4. Individually fair representations of high-dimensional data

Our method defines a set $S(\mathbf{x})$ of individuals similar to \mathbf{x} (Sec. 4.1), learns individually fair representations of these individuals (Sec. 4.2) and finally, certifies individual fairness for them (Sec. 4.3). The approach is general, but for presentational purposes we focus on images.

4.1. Similarity via a generative model

We consider two individuals \mathbf{x} and \mathbf{x}' to be similar if they differ only in their sensitive attributes while the other attributes are the same. However, semantic attributes, such as skin color, cannot be conveniently captured directly in the input features of \mathbf{x} . Our key idea is to leverage a generative model G and define similarity in its latent space. We then compute a vector \mathbf{a} associated with the sensitive attribute, such that interpolating along the direction of \mathbf{a} in the latent space and reconstructing back to the input space results in a

meaningful semantic transformation of that attribute. This in itself is an active research area and various approaches for computing \mathbf{a} exist [15, 32].

Individual similarity via Glow

In this work, we define individual similarity in the latent space of Glow [42]. Let $\mathbf{z}_G = E_G(\mathbf{x})$ be the latent code of \mathbf{x} in the generative model latent space. Kingma and Dhariwal [42] observed that we can compute \mathbf{a} by calculating the average latent vectors $\mathbf{z}_{G,pos}$ for samples with the attribute and $\mathbf{z}_{G,neg}$ for samples without it, and setting \mathbf{a} to their difference: $\mathbf{a} = \mathbf{z}_{G,pos} - \mathbf{z}_{G,neg}$. Then, moving in the direction of \mathbf{a} in the latent space increases the presence of the attribute and interpolating in the opposite direction decreases it. Once we have G and \mathbf{a} , we define the set of individuals similar to \mathbf{x} in the latent space of G to be $S(\mathbf{x}) = \{\mathbf{z}_G + t \cdot \mathbf{a} \mid t \in [-\epsilon, \epsilon]\}$ (see top of Fig. 2). Here, ϵ defines the maximum perturbation level that we can apply to the attribute. We consider G , \mathbf{a} and ϵ to be a part of the similarity specification set by the data regulator. Crucially, the similarity set $S(\mathbf{x})$ contains an infinite number of points, but is compactly represented in the latent space of G as a line segment. In contrast, the same set represented directly in the input space, $S_i(\mathbf{x}) := \{D_G(\mathbf{z}) \mid \mathbf{z} \in S(\mathbf{x})\}$, obtained by decoding the latent representations in $S(\mathbf{x})$, cannot be abstracted conveniently without additional information (see bottom of Fig. 2). Moreover, this approach for constructing $S(\mathbf{x})$ can also be extended to multiple sensitive attributes by interpolating along their attribute vectors simultaneously.

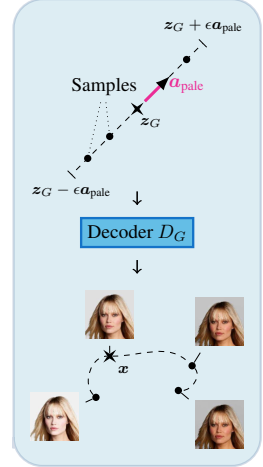


Figure 2. Similarity

Once we have G and \mathbf{a} , we define the set of individuals similar to \mathbf{x} in the latent space of G to be $S(\mathbf{x}) = \{\mathbf{z}_G + t \cdot \mathbf{a} \mid t \in [-\epsilon, \epsilon]\}$ (see top of Fig. 2). Here, ϵ defines the maximum perturbation level that we can apply to the attribute. We consider G , \mathbf{a} and ϵ to be a part of the similarity specification set by the data regulator. Crucially, the similarity set $S(\mathbf{x})$ contains an infinite number of points, but is compactly represented in the latent space of G as a line segment. In contrast, the same set represented directly in the input space, $S_i(\mathbf{x}) := \{D_G(\mathbf{z}) \mid \mathbf{z} \in S(\mathbf{x})\}$, obtained by decoding the latent representations in $S(\mathbf{x})$, cannot be abstracted conveniently without additional information (see bottom of Fig. 2). Moreover, this approach for constructing $S(\mathbf{x})$ can also be extended to multiple sensitive attributes by interpolating along their attribute vectors simultaneously.

4.2. Learning individually fair representations

Assuming that the generative model $G = D_G \circ E_G$ is pretrained and given, in this section we describe the training of the encoder $L : \mathbb{R}^n \rightarrow \mathbb{R}^k$. Together with G , it forms the data producer of our end-to-end model. To simplify the notation, we define $P = L \circ D_G$, mapping from the latent space of G to the latent space of L . L is trained separately from the data consumer, the classifier C , the training of which is explained in the next section.

Adversarial loss We encourage similar treatment for all points in $S_i(\mathbf{x})$ by training L to map them close to each

other in \mathbb{R}^k . This can be achieved by minimizing the loss

$$\mathcal{L}_{adv}(\mathbf{x}) = \max_{z' \in S(\mathbf{x})} \|P(z_G) - P(z')\|_2. \quad (3)$$

Minimizing $\mathcal{L}_{adv}(\mathbf{x})$ is a min-max optimization problem and adversarial training [54] has been demonstrated to work well in such setups. Because the underlying domain of the inner maximization problem is simply the line segment $S(\mathbf{x})$, we perform a random adversarial attack in which we sample s points $z_i \sim \mathcal{U}(S(\mathbf{x}))$ uniformly at random from $S(\mathbf{x})$ and approximate $\mathcal{L}_{adv}(\mathbf{x}) \approx \max_{i=1}^s \|P(z_G) - P(z_i)\|_2$. This efficient attack is typically more effective [19] than the first-order methods such as FGSM [26] and PGD [54] when the search space is low-dimensional.

Classification loss To learn representations useful for downstream tasks, we train L jointly with an auxiliary classifier C_{aux} to predict a ground-truth target label y by adding an additional term to the loss function:

$$\mathcal{L}_{cls}(\mathbf{x}, y) = \text{cross_entropy}((C_{aux} \circ P)(z_G), y). \quad (4)$$

Contrastive loss In theory, we can make \mathcal{L}_{adv} arbitrarily small while preserving \mathcal{L}_{cls} by dividing the output of L and multiplying the input of C by a large constant, pushing all points $P(z)$ close to each other regardless of their ground-truth class y . Having points with different classes close to each other reduces the confidence of C during smoothing and can result in a smaller certified radius, which has implications for the certification method proposed in Sec. 4.3. To prevent this from happening and to promote better separability of the classes, we consider a modification of the contrastive loss [10]. Denoting $d(\mathbf{x}_i, \mathbf{x}_j) = \|L(\mathbf{x}_i) - L(\mathbf{x}_j)\|_2$, we define the contrastive loss for a mini-batch $\mathcal{B} = \{(\mathbf{x}_i, y_i)\}_{i=1}^b$:

$$\mathcal{L}_{contr}(\mathcal{B}) = \sum_{i,j} \mathbb{I}[y_i = y_j] \max(0, d(\mathbf{x}_i, \mathbf{x}_j) - \delta) + \mathbb{I}[y_i \neq y_j] \max(0, 2\delta - d(\mathbf{x}_i, \mathbf{x}_j)) \quad (5)$$

where $\mathbb{I}[\cdot]$ is the indicator function and δ is a hyperparameter. The loss term penalizes pairs of inputs from the same class encoded further than δ from each other and pairs from different classes encoded closer than 2δ from each other. In the end, L is trained jointly with C_{aux} using stochastic gradient descent. The total loss for each mini-batch \mathcal{B} is

$$\frac{1}{b} \sum_{i=1}^b (\mathcal{L}_{cls}(\mathbf{x}_i, y_i) + \lambda_1 \mathcal{L}_{adv}(\mathbf{x})) + \frac{\lambda_2}{b^2} \mathcal{L}_{contr}(\mathcal{B}) \quad (6)$$

with λ_1 and λ_2 being hyperparameters balancing the adversarial and contrastive loss with the classification loss. Trading off fairness and accuracy, viewed as a multi-objective optimization problem, is an active area of research. Here we follow prior work [53, 65] and use linear weighting, but we remark that other schemes are also possible.

Algorithm 1 Certifying the individual fairness of $\widehat{C} \circ \widehat{P} \circ E_G$ for the input \mathbf{x} .

function CERTIFY($E_G, D_G, L, C, \mathbf{x}$)

Let $z_G = E_G(\mathbf{x})$ and $P = L \circ D_G$.

$z_{cs} = \widehat{P}(z_G)$ and r_{cs} from center smoothing [45].

if center smoothing abstained **then return** ABSTAIN
Smooth C [11] to obtain the certified radius R around z_{cs} for which the classification stays the same.

if $r_{cs} < R$ **then return** CERTIFIED

else return NOT CERTIFIED

4.3. Certifying individual fairness via latent space smoothing

So far, we have a pretrained generative model $G = D_G \circ E_G$, which allows us to compute the attribute vector \mathbf{a} . $S(\mathbf{x})$ and in turn $S_i(\mathbf{x})$ are defined based on \mathbf{a} and the maximum perturbation level ϵ . Assume that we have trained L as discussed above, as well as C , the training of which is described at the end of this section. We now construct the end-to-end model M for which, given an input \mathbf{x} , we can certify individual fairness of the form

$$\forall \mathbf{x}' \in S_i(\mathbf{x}). M(\mathbf{x}) = M(\mathbf{x}'). \quad (7)$$

Assume that we have a point $z \in \mathbb{R}^q$ in the latent space of G and define the function $g_z(t) = P(z + t \cdot \mathbf{a})$, $t \in \mathbb{R}$. We apply the center smoothing procedure presented by Kumar and Goldstein [45] to obtain the smoothed version of g_z , namely \widehat{g}_z , and define $\widehat{P}(z) = \widehat{g}_z(0)$, such that for all $z' \in S(\mathbf{x})$, $\|\widehat{P}(z) - \widehat{P}(z')\|_2 \leq r_{cs}$ (Thm. 3.2, see Fig. 3). Moreover, we smooth the classifier C to derive the end-to-end model $M = \widehat{C} \circ \widehat{P} \circ E_G$ which can be certified with high probability. The compositional certification procedure is summarized in Alg. 1 and its correctness is given by Thm. 4.1. A detailed proof is in App. A.

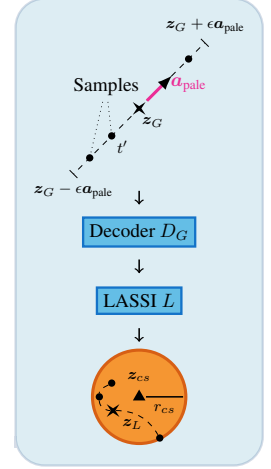


Figure 3. Center smoothing

Theorem 4.1. Assume that we have a bijective generative model $G = D_G \circ E_G$ used to define the similarity set $S_i(\mathbf{x})$ for a given input \mathbf{x} . Let Alg. 1 perform center smoothing [45] with confidence $1 - \alpha_c$ and classification smoothing [11] with confidence $1 - \alpha_s$. If Alg. 1 returns CERTIFIED for the input \mathbf{x} , then the end-to-end model $M = \widehat{C} \circ \widehat{P} \circ E_G$

is individually fair for \mathbf{x} w.r.t. $S_i(\mathbf{x})$ with probability at least $1 - \alpha_c - \alpha_s$.

Training C Because we will be applying smoothing over the classifier C , following Cohen et al. [11], once we have trained L , we train C separately by adding isotropic Gaussian noise to its inputs during the training process. The inputs of C here are the outputs of $L \circ D_G \circ E_G$. We do not smooth the pipeline at this step as it is computationally expensive and because the distance between the smoothed and the unsmoothed outputs is generally small [45].

5. Experiments

We now present experimental evaluation of LASSI. Our key findings are that: (i) LASSI reliably enforces individual fairness and keeps accuracy high, (ii) LASSI is applicable to a wide range of sensitive attributes, (iii) guarantees of LASSI obtained using generative models can transfer to real-world.

Datasets We evaluate LASSI on three datasets. CelebA¹ [50] (restricted to non-commercial research and education purposes; Liu et al. [50] do not own the copyrights) contains 202,599 aligned and cropped face images of real-world celebrities. The images are annotated with the presence or absence of 40 face attributes with various correlations between them [15]. As CelebA is highly imbalanced, we also experiment with FairFace [36] (License: CC BY 4.0), which is balanced on race and contains 97,698 released images (we use padding 0.25) of individuals from 7 race and 9 age groups. We split the training set randomly in ratio 80:20 for development and evaluate on the validation set because the test set is not publicly shared. Finally, the 3D Shapes dataset [8] (License: Apache-2.0) consists of images of 3D shapes that are procedurally generated from 6 independent latent factors: floor hue, wall hue, object hue, scale, and orientation. The 3D Shapes dataset is typically used to investigate disentanglement properties of unsupervised learning methods (e.g., in the context of fairness [51]).

Experimental setup The following setup is used for all experiments, unless stated otherwise. We use images of size 64×64 , and for each dataset we pretrain a Glow model G with 4 blocks of 32 flows, using an open-source PyTorch [62] implementation [69]. We set $\epsilon = 1$ such that $S_i(\mathbf{x})$ contains realistic high-quality reconstructions. Thus, similarity specification used to enforce individual fairness is determined by the generative model G and radius ϵ . We use ResNet-18 [30] for the LASSI encoder L with its final fully-connected layer replaced by zero mean and unit variance

normalization ensuring that all components of the output of L are in the same range when Gaussian noise is added during smoothing. We use a linear classifier C for predicting the target label.

Our fairness-unaware baseline (referred to as Naive below) is standard representation learning of L ($\lambda_1 = \lambda_2 = 0$), corresponding to cross-entropy training. After evaluating the baseline with $\sigma_{enc} \in \{0.5, 0.75, 1\}$, we set $\sigma_{enc} = 0.75$ as it performed slightly better in all initial experiments. We did a careful hyperparameter search over λ_1 , λ_2 and δ on CelebA, predicting Smiling with sensitive attribute Pale_Skin (see App. B for details on the hyperparameter search) and selected $\lambda_1 = \lambda_2 = 0.1$, $\delta = 50$ for the LASSI model. λ_1 controls the trade-off between fairness and accuracy, and adding the contrastive loss consistently outperformed training only with classification and adversarial losses (we demonstrate this using an ablation study in App. D). We considered 9 different levels of Gaussian noise for C : $\sigma_{cls} \in \{0.1, 0.25, 0.5\} \times 1e\{0, 1, 2\}$ and selected $\sigma_{cls} = 10$ for the Naive and LASSI models, but reduced it for imbalanced or more difficult tasks so that we do not add excessive noise to the classifier. In App. B we demonstrate that LASSI works for a wide range of hyperparameter values. For scalability reasons, we drew $s = 5$ random samples to approximate \mathcal{L}_{adv} , slowing down the training $7 \times$ in total, compared to Naive. Following prior work on smoothing [11, 45], we set $\alpha_c = 0.01$ and $\alpha_s = 0.001$. We ran the experiments on GeForce RTX 2080 Ti GPUs and will release all the code and models to reproduce our results.

Single sensitive attribute We experiment with 4 different continuous sensitive attributes from CelebA: Pale_Skin, Young, Blond_Hair and Heavy_Makeup on two tasks: predicting Smiling and Wearing_Earrings. We chose attributes with different balance ratios which have also been used in prior work [15], while avoiding attributes that perpetuate harmful stereotypes [15] (e.g., avoiding Male). Glow can also be used to generate discrete attributes, but then fairness certification can be done via enumeration because partial eyeglasses or hats, for example, are not plausible. Fig. 4 provides example images from $S_i(\mathbf{x})$ for a single \mathbf{x} . Wearing_Earrings is considerably more imbalanced than Smiling, with the majority class obtaining 78.21% accuracy on our test subset, so we used $\sigma_{cls} = 5$ for Naive (but kept $\sigma_{cls} = 10$ for LASSI) for that task.

In a recent work, Ramaswamy et al. [64] proposed generating synthetic images with a GAN [27] to balance the dataset. Their method is not concerned with individual fairness and their transformation of latent representations may change other, non-sensitive attributes. Nevertheless, we compare with a similar data augmentation strategy randomly sampling s additional images from $S_i(\mathbf{x})$ for each

¹<https://mmlab.ie.cuhk.edu.hk/projects/CelebA.html>

Task	Sensitive attribute(s)	Naive		Data Aug. [64]		LASSI (ours)	
		Acc. (%)	Fair (%)	Acc. (%)	Fair (%)	Acc. (%)	Fair (%)
Smiling	Pale_Skin	92.31	7.69	91.67	16.03	90.38	75.64
	Young	92.95	22.44	91.67	23.08	92.95	82.05
	Blond_Hair	92.95	21.79	92.31	30.77	91.67	83.97
	Heavy_Makeup	93.59	11.54	91.03	7.69	91.03	76.92
	Pale + Young	92.31	2.56	88.46	12.18	89.74	66.67
	Pale + Young + Blond	92.95	1.28	93.59	4.49	89.74	57.05
Earrings	Pale_Skin	83.33	8.97	84.62	16.67	87.18	71.15
	Young	83.97	2.56	83.33	12.82	82.05	67.31
	Blond_Hair	83.97	0.64	82.05	12.18	82.05	72.44
	Heavy_Makeup	83.97	0.64	82.69	4.49	78.21	82.05

Table 1. Evaluation of LASSI on the CelebA dataset, showing that LASSI significantly increases certified individual fairness compared to the baselines without affecting the classification accuracy.



Figure 4. Similar points from $S_i(\mathbf{x})$, as reconstructed by Glow, for multiple combinations of sensitive attributes. Central images correspond to the original input. We vary t uniformly (from left to right) in the $[-\frac{\epsilon}{\sqrt{n}}, \frac{\epsilon}{\sqrt{n}}]$ range, n = number of sensitive attributes, $\epsilon = 1$. For $n > 1$, all attribute vectors are multiplied by the same t .

training sample. We empirically set $\sigma_{cls} = 5$ for this baseline. We do not compare with LCIFR [65] as its certification is based on expensive solvers that do not scale to Glow and ResNet.

We show the results in Tab. 1, measured on a subset of

Sensitive attribute	Naive		LASSI (ours)	
	Acc. (%)	Fair (%)	Acc. (%)	Fair (%)
Pale_Skin	91.67	24.36	91.67	78.85
Young	92.31	46.79	91.67	83.97

Table 2. Results on 128×128 -dimensional CelebA images. Target attribute is Smiling.

156 samples from CelebA’s test set. Certifying each sample (Alg. 1) takes up to 3 minutes, the bottleneck being center smoothing through the Glow decoder. For each input point \mathbf{x} , we are interested if the prediction of the end-to-end model M matches the ground-truth and if Alg. 1 returns CERTIFIED. The results show that data augmentation helps, but is not enough – LASSI significantly improves the certified fairness, compared to the baselines, with a minor loss of accuracy, for both Smiling and Wearing_Earrings tasks. Heavy_Makeup converges to predicting the majority class for Earrings. The hardness of this configuration confirms the high correlation between the two in the data (in fact, Heavy_Makeup is the third attribute most highly correlated with Earrings).

Multiple sensitive attributes We now combine the sensitive attributes Pale_Skin, Young and Blond_Hair and predict Smiling. The similarity sets w.r.t. which we certify individual fairness are defined as $S(\mathbf{x}) = \{E_G(\mathbf{x}) + \sum_i t_i \cdot \mathbf{a}_i \mid \sqrt{\sum_i t_i^2} \leq \epsilon\}$, i.e., $\|\mathbf{t}\|_2 \leq \epsilon$ for the vector of coefficients (t_1, t_2, \dots) . To accommodate for the bigger similarity sets, we set $s = 10$ when combining two sensitive attributes and $s = 15$ when we combine three. The results in Tab. 1 (rows 5 – 6) show that LASSI also successfully enforces individual fairness in this case.

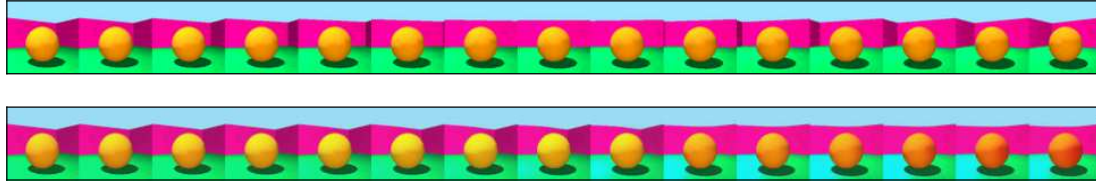


Figure 5. A sample shape at 15 different ground truth orientations (top) and the corresponding reconstructions obtained from interpolating along the generative model’s attribute vector (bottom), showing that generative model is close to ground truth.

Method	Acc. (%)	Fair (%)	Unfair (%)
Naive	92.67	0	44.67
LASSI (ours)	100	88	0

Table 3. Evaluation on the 3D shapes for the task `object hue` and sensitive attribute `orientation`. Certification using the generative model transfers to ground truth data as the certification rate and percentage of unfair ground truth data sum up below 100%.

Larger images Next, we explore if LASSI can also work with larger images. We increase the dimensionality of the CelebA images to 128×128 , pretrain Glow with 5 blocks, and train and certify LASSI on 4 GPUs in parallel to keep the certification time the same. The results in Tab. 2 show that larger images are actually more certifiable for individual fairness. This is likely because they are of a higher quality and the model receives more signal in order to make more confident classifications.

Training on FairFace dataset To verify that the root cause for the individual unfairness is algorithmic and not dataset specific, we evaluate our method on the balanced FairFace [36] dataset. We select `Race=Black` as a sensitive attribute and predict `Age`. This is a very challenging multi-class task with around 60% state of the art accuracy. We report results on 172 test samples with $\epsilon = 0.5$, $\sigma_{enc} = 0.375$, $\sigma_{cls} = 2.5$ and $\lambda_2 = 0.05$, $\delta = 25$ to leave enough capacity to the model. L is originally pretrained on ImageNet [14]. Naive obtains 45.93% accuracy and 6.4% certified fairness, while LASSI has 45.35% and 20.35% respectively, demonstrating that LASSI can significantly improve the certified individual fairness even in the balanced data setting.

Certification with ground truth data An essential part of the evaluation is demonstrating that the fairness certificates obtained using the generative model transfer to ground truth data. Since CelebA does not contain images of the same individual with different attributes, *e.g.*, the same individual with different skin colors, we use the 3D Shapes

dataset [8], which provides images of the same object with varying latent factors. The goal is to show that the attribute vector computed by Glow captures a given latent factor (as in Fig. 5), and thus certification with respect to the similarity set defined by that attribute vector will result in certification of the ground truth. To that end, we consider `orientation` as the continuous sensitive attribute, since it has 15 different values, which is the most of all the latent factors, and thus provides the most rigorous evaluation. We obtain 15 similar ground truth data points, *i.e.*, the same shape at 15 different orientations (fixing all other factors). Here, for every certified data point from the test set, we check whether all 15 similar ground truth data points obtain the same classification, indicating ground truth fairness. For `object hue` classification, Tab. 3 demonstrates that LASSI achieves 100% accuracy and 88% certified fairness on this task (using Glow), while being 100% fair on the ground truth images, showing that the certificates transfer to the ground truth.

6. Limitations

While LASSI captures semantic transformations using a generative model, this could only include a subset of inputs that are semantically similar to a human observer. Moreover, certificates obtained using generative models may not always transfer to the real world (this was to some extent investigated with 3D Shapes in Sec. 5). In this work, we restricted ourselves to parametrized lines in latent space, but there might be other similarity definitions that cannot be captured by a line. Lastly, smoothing can be time consuming during inference and certification, especially for large models.

7. Conclusion

We defined image similarity with respect to a generative model via attribute manipulation, allowing us to capture complex image transformations such as changing the age or skin color, which are otherwise difficult to characterize. Further, we were able to scale certified representation learning for individual fairness to real world high dimensional datasets by using randomized smoothing based techniques.

Our extensive evaluation yields promising results on several datasets and illustrates the practicality of our approach.

Ethics statement

Certified individual fairness is important for the reliable deployment of machine learning systems in real world applications and is required by regulators. As this work certifies individual fairness with respect to a generative model approximating the ground truth, potential biases encoded in the generative model can prevail and skew certification. However, quality advancements in generative models can directly translate into stronger guarantees of our method, enabling certified fair application of models which use rich, high dimensional data.

Acknowledgments

We would like to thank Seyedmorteza Sadat for his help with initial investigations in enforcing fairness in the latent space of a generative model. We are also grateful to the anonymous reviewers for their insightful comments and suggestions.

References

- [1] Aws Albarghouthi, Loris D’Antoni, Samuel Drews, and Aditya V. Nori. Fairsquare: probabilistic verification of program fairness. *Proc. ACM Program. Lang.*, 2017. 3
- [2] Guha Balakrishnan, Yuanjun Xiong, Wei Xia, and Pietro Perona. Towards causal benchmarking of bias in face analysis algorithms. In *Computer Vision - ECCV 2020 - 16th European Conference*, 2020. 3
- [3] Mislav Balunovic, Anian Ruoss, and Martin T. Vechev. Fair normalizing flows. *CoRR*, 2021. 3
- [4] Osbert Bastani, Xin Zhang, and Armando Solar-Lezama. Probabilistic verification of fairness properties via concentration. *Proc. ACM Program. Lang.*, 2019. 3
- [5] Tolga Bolukbasi, Kai-Wei Chang, James Y. Zou, Venkatesh Saligrama, and Adam Tauman Kalai. Man is to computer programmer as woman is to homemaker? debiasing word embeddings. In *Advances in Neural Information Processing Systems 29*, 2016. 3
- [6] Tim Brennan, William Dieterich, and Beate Ehret. Evaluating the predictive validity of the compas risk and needs assessment system. *Criminal Justice and Behavior*, 2009. 1
- [7] Joy Buolamwini and Timnit Gebru. Gender shades: Intersectional accuracy disparities in commercial gender classification. In *Conference on Fairness, Accountability and Transparency*, 2018. 1, 3
- [8] Chris Burgess and Hyunjik Kim. 3d shapes dataset. <https://github.com/deepmind/3dshapes-dataset/>, 2018. 6, 8
- [9] YooJung Choi, Meihua Dang, and Guy Van den Broeck. Group fairness by probabilistic modeling with latent fair decisions. In *Thirty-Fifth AAAI Conference on Artificial Intelligence*, 2021. 3
- [10] Sumit Chopra, Raia Hadsell, and Yann LeCun. Learning a similarity metric discriminatively, with application to face verification. In *IEEE Computer Society Conference on Computer Vision and Pattern Recognition*, 2005. 5
- [11] Jeremy M. Cohen, Elan Rosenfeld, and J. Zico Kolter. Certified adversarial robustness via randomized smoothing. In *Proceedings of the 36th International Conference on Machine Learning*, 2019. 1, 2, 3, 4, 5, 6, 13
- [12] Elliot Creager, David Madras, Jörn-Henrik Jacobsen, Marissa A. Weis, Kevin Swersky, Toniann Pitassi, and Richard S. Zemel. Flexibly fair representation learning by disentanglement. In *Proceedings of the 36th International Conference on Machine Learning*, 2019. 3
- [13] Saloni Dash and Amit Sharma. Counterfactual generation and fairness evaluation using adversarially learned inference. *CoRR*, 2020. 3
- [14] Jia Deng, Wei Dong, Richard Socher, Li-Jia Li, Kai Li, and Li Fei-Fei. Imagenet: A large-scale hierarchical image database. In *2009 IEEE Conference on Computer Vision and Pattern Recognition*, pages 248–255, 2009. 8
- [15] Emily Denton, Ben Hutchinson, Margaret Mitchell, and Timnit Gebru. Detecting bias with generative counterfactual face attribute augmentation. *CoRR*, 2019. 3, 4, 6
- [16] Cynthia Dwork, Moritz Hardt, Toniann Pitassi, Omer Reingold, and Richard S. Zemel. Fairness through awareness. In *Innovations in Theoretical Computer Science*, 2012. 2
- [17] Harrison Edwards and Amos J. Storkey. Censoring representations with an adversary. In *4th International Conference on Learning Representations*, 2016. 3
- [18] Rüdiger Ehlers. Formal verification of piece-wise linear feed-forward neural networks. In *Automated Technology for Verification and Analysis - 15th International Symposium*, 2017. 1
- [19] Logan Engstrom, Brandon Tran, Dimitris Tsipras, Ludwig Schmidt, and Aleksander Madry. Exploring the landscape of spatial robustness. In Kamalika Chaudhuri and Ruslan Salakhutdinov, editors, *Proceedings of the 36th International Conference on Machine Learning*, volume 97 of *Proceedings of Machine Learning Research*, pages 1802–1811. PMLR, 09–15 Jun 2019. 5
- [20] EU. Ethics guidelines for trustworthy ai, 2019. 1, 3
- [21] EU. Proposal for a regulation of the european parliament and of the council laying down harmonised rules on artificial intelligence (artificial intelligence act) and amending certain union legislative acts, 2021. 1, 3
- [22] Rui Feng, Yang Yang, Yuehan Lyu, Chenhao Tan, Yizhou Sun, and Chunping Wang. Learning fair representations via an adversarial framework. *CoRR*, 2019. 3
- [23] FTC. Using artificial intelligence and algorithms, 2020. 1, 3
- [24] FTC. Aiming for truth, fairness, and equity in your company’s use of ai, 2021. 1, 3
- [25] Xavier Gitiaux and Huzefa Rangwala. Learning smooth and fair representations. In *The 24th International Conference on Artificial Intelligence and Statistics*, 2021. 1, 3
- [26] Ian Goodfellow, Jonathon Shlens, and Christian Szegedy. Explaining and harnessing adversarial examples. In *International Conference on Learning Representations*, 2015. 5
- [27] Ian J. Goodfellow, Jean Pouget-Abadie, Mehdi Mirza, Bing Xu, David Warde-Farley, Sherjil Ozair, Aaron C. Courville, and Yoshua Bengio. Generative adversarial nets. In *Advances in Neural Information Processing Systems 27*, 2014. 3, 6
- [28] Sven Gowal, Chongli Qin, Po-Sen Huang, A. Taylan Cemgil, Krishnamurthy Dvijotham, Timothy A. Mann, and Pushmeet Kohli. Achieving robustness in the wild via adversarial mixing with disentangled representations. In *CVPR*, pages 1208–1217. Computer Vision Foundation / IEEE, 2020. 3
- [29] Moritz Hardt, Eric Price, and Nati Srebro. Equality of opportunity in supervised learning. In *Advances in Neural Information Processing Systems 29*, 2016. 2
- [30] Kaiming He, Xiangyu Zhang, Shaoqing Ren, and Jian Sun. Deep residual learning for image recognition. In *IEEE Conference on Computer Vision and Pattern Recognition*, 2016. 6
- [31] Lisa Anne Hendricks, Kaylee Burns, Kate Saenko, Trevor Darrell, and Anna Rohrbach. Women also snowboard: Overcoming bias in captioning models. In *Computer Vision - ECCV 2018 - 15th European Conference*, 2018. 3
- [32] Irina Higgins, Loïc Matthey, Arka Pal, Christopher Burgess,

- Xavier Glorot, Matthew Botvinick, Shakir Mohamed, and Alexander Lerchner. beta-vae: Learning basic visual concepts with a constrained variational framework. In *5th International Conference on Learning Representations*, 2017. 4
- [33] Christina Ilvento. Metric learning for individual fairness. In *1st Symposium on Foundations of Responsible Computing*, 2020. 2
- [34] Philips George John, Deepak Vijaykeerthy, and Diptikalyan Saha. Verifying individual fairness in machine learning models. In *Proceedings of the Thirty-Sixth Conference on Uncertainty in Artificial Intelligence*, 2020. 3
- [35] Jungseock Joo and Kimmo Kärkkäinen. Gender slopes: Counterfactual fairness for computer vision models by attribute manipulation. *CoRR*, 2020. 3
- [36] Kimmo Karkkainen and Jungseock Joo. Fairface: Face attribute dataset for balanced race, gender, and age for bias measurement and mitigation. In *Proceedings of the IEEE/CVF Winter Conference on Applications of Computer Vision*, pages 1548–1558, 2021. 6, 8
- [37] Michael J. Kearns, Seth Neel, Aaron Roth, and Zhiwei Steven Wu. Preventing fairness gerrymandering: Auditing and learning for subgroup fairness. In *Proceedings of the 35th International Conference on Machine Learning*, 2018. 2
- [38] Thomas Kehrenberg, Myles Bartlett, Oliver Thomas, and Novi Quadrianto. Null-sampling for interpretable and fair representations. In *Computer Vision - ECCV 2020 - 16th European Conference*, 2020. 3
- [39] Amir E. Khandani, Adlar J. Kim, and Andrew W. Lo. Consumer credit-risk models via machine-learning algorithms. *Journal of Banking & Finance*, 2010. 1
- [40] Been Kim, Martin Wattenberg, Justin Gilmer, Carrie J. Cai, James Wexler, Fernanda B. Viégas, and Rory Sayres. Interpretability beyond feature attribution: Quantitative testing with concept activation vectors (TCAV). In *Proceedings of the 35th International Conference on Machine Learning*, 2018. 3
- [41] Hyemi Kim, Seungjae Shin, JoonHo Jang, Kyungwoo Song, Weonyoung Joo, Wanmo Kang, and Il-Chul Moon. Counterfactual fairness with disentangled causal effect variational autoencoder. In *Thirty-Fifth AAAI Conference on Artificial Intelligence*, 2021. 3
- [42] Diederik P. Kingma and Prafulla Dhariwal. Glow: Generative flow with invertible 1x1 convolutions. In *Advances in Neural Information Processing Systems 31*, 2018. 1, 3, 4
- [43] Diederik P. Kingma and Max Welling. Auto-encoding variational bayes. In *2nd International Conference on Learning Representations*, 2014. 3
- [44] Brendan Klare, Mark James Burge, Joshua C. Klontz, Richard W. Vorder Bruegge, and Anil K. Jain. Face recognition performance: Role of demographic information. *IEEE Trans. Inf. Forensics Secur.*, 2012. 1, 3
- [45] Aounon Kumar and Tom Goldstein. Center smoothing: Certified robustness for networks with structured outputs. *Advances in Neural Information Processing Systems 34*, 2021. 1, 2, 4, 5, 6, 13
- [46] Preethi Lahoti, Krishna P. Gummadi, and Gerhard Weikum. ifair: Learning individually fair data representations for algorithmic decision making. In *35th IEEE International Conference on Data Engineering*, 2019. 3
- [47] Preethi Lahoti, Krishna P. Gummadi, and Gerhard Weikum. Operationalizing individual fairness with pairwise fair representations. *Proc. VLDB Endow.*, 2019. 3
- [48] Paul Pu Liang, Chiyu Wu, Louis-Philippe Morency, and Ruslan Salakhutdinov. Towards understanding and mitigating social biases in language models. In *Proceedings of the 38th International Conference on Machine Learning*, 2021. 3
- [49] Jiachun Liao, Chong Huang, Peter Kairouz, and Lalitha Sankar. Learning generative adversarial representations (GAP) under fairness and censoring constraints. *CoRR*, 2019. 3
- [50] Ziwei Liu, Ping Luo, Xiaogang Wang, and Xiaoou Tang. Deep learning face attributes in the wild. In *IEEE International Conference on Computer Vision*, 2015. 6
- [51] Francesco Locatello, Gabriele Abbati, Thomas Rainforth, Stefan Bauer, Bernhard Schölkopf, and Olivier Bachem. On the fairness of disentangled representations. In *Advances in Neural Information Processing Systems 32*, 2019. 3, 6
- [52] Christos Louizos, Kevin Swersky, Yujia Li, Max Welling, and Richard S. Zemel. The variational fair autoencoder. In *4th International Conference on Learning Representations*, 2016. 3
- [53] David Madras, Elliot Creager, Toniann Pitassi, and Richard S. Zemel. Learning adversarially fair and transferable representations. In *Proceedings of the 35th International Conference on Machine Learning*, 2018. 3, 5
- [54] Aleksander Madry, Aleksandar Makelov, Ludwig Schmidt, Dimitris Tsipras, and Adrian Vladu. Towards deep learning models resistant to adversarial attacks. In *6th International Conference on Learning Representations*, 2018. 2, 5
- [55] Subha Maity, Songkai Xue, Mikhail Yurochkin, and Yuekai Sun. Statistical inference for individual fairness. In *9th International Conference on Learning Representations*, 2021. 2
- [56] Daniel J. McDuff, Roger Cheng, and Ashish Kapoor. Identifying bias in AI using simulation. *CoRR*, 2018. 3
- [57] Daniel McNamara, Cheng Soon Ong, and Robert C. Williamson. Costs and benefits of fair representation learning. In *Proceedings of the 2019 AAAI/ACM Conference on AI, Ethics, and Society*, 2019. 1
- [58] Matthew Mirman, Alexander Hägele, Pavol Bielik, Timon Gehr, and Martin T. Vechev. Robustness certification with generative models. In *PLDI*, pages 1141–1154. ACM, 2021. 3
- [59] Debarghya Mukherjee, Mikhail Yurochkin, Moulinath Banerjee, and Yuekai Sun. Two simple ways to learn individual fairness metrics from data. In *Proceedings of the 37th International Conference on Machine Learning*, 2020. 2
- [60] Luca Oneto, Michele Donini, Massimiliano Pontil, and Andreas Maurer. Learning fair and transferable representations with theoretical guarantees. In *7th IEEE International Conference on Data Science and Advanced Analytics*, 2020. 3
- [61] Ji Ho Park, Jamin Shin, and Pascale Fung. Reducing gender bias in abusive language detection. In *Proceedings of the 2018 Conference on Empirical Methods in Natural Language Processing*, 2018. 3
- [62] Adam Paszke, Sam Gross, Francisco Massa, Adam Lerer,

- James Bradbury, Gregory Chanan, Trevor Killeen, Zeming Lin, Natalia Gimelshein, Luca Antiga, Alban Desmaison, Andreas Köpf, Edward Z. Yang, Zachary DeVito, Martin Raison, Alykhan Tejani, Sasank Chilamkurthy, Benoit Steiner, Lu Fang, Junjie Bai, and Soumith Chintala. Pytorch: An imperative style, high-performance deep learning library. In Hanna M. Wallach, Hugo Larochelle, Alina Beygelzimer, Florence d’Alché-Buc, Emily B. Fox, and Roman Garnett, editors, *Advances in Neural Information Processing Systems 32: Annual Conference on Neural Information Processing Systems 2019, NeurIPS 2019, December 8-14, 2019, Vancouver, BC, Canada*, pages 8024–8035, 2019. 6
- [63] Inioluwa Deborah Raji and Joy Buolamwini. Actionable auditing: Investigating the impact of publicly naming biased performance results of commercial AI products. In *Proceedings of the 2019 AAAI/ACM Conference on AI, Ethics, and Society*, 2019. 3
- [64] Vikram V. Ramaswamy, Sunnie S. Y. Kim, and Olga Russakovsky. Fair attribute classification through latent space de-biasing. In *IEEE Conference on Computer Vision and Pattern Recognition*, 2021. 3, 6, 7
- [65] Anian Ruoss, Mislav Balunovic, Marc Fischer, and Martin T. Vechev. Learning certified individually fair representations. In *Advances in Neural Information Processing Systems 33*, 2020. 1, 3, 5, 7
- [66] Mhd Hasan Sarhan, Nassir Navab, Abouzar Eslami, and Shadi Albarqouni. Fairness by learning orthogonal disentangled representations. In *Computer Vision - ECCV 2020 - 16th European Conference*, 2020. 3
- [67] Prasanna Sattigeri, Samuel C. Hoffman, Vijil Chenthamarakshan, and Kush R. Varshney. Fairness GAN: generating datasets with fairness properties using a generative adversarial network. *IBM J. Res. Dev.*, 2019. 3
- [68] Shahar Segal, Yossi Adi, Benny Pinkas, Carsten Baum, Chaya Ganesh, and Joseph Keshet. Fairness in the eyes of the data: Certifying machine-learning models. In *AAAI/ACM Conference on AI, Ethics, and Society*, 2021. 3
- [69] Kim Seonghyeon. Glow pytorch (commit: 97081ff1). <https://github.com/rosinality/glow-pytorch>, 2020. 6
- [70] Jiaming Song, Pratyusha Kalluri, Aditya Grover, Shengjia Zhao, and Stefano Ermon. Learning controllable fair representations. In *The 22nd International Conference on Artificial Intelligence and Statistics*, 2019. 3
- [71] Xudong Sun, Pengcheng Wu, and Steven CH Hoi. Face detection using deep learning: An improved faster rcnn approach. *Neurocomputing*, 299:42–50, 2018. 1
- [72] Rachael Tatman. Gender and dialect bias in youtube’s automatic captions. In *Proceedings of the First ACL Workshop on Ethics in Natural Language Processing*, 2017. 3
- [73] Vincent Tjeng, Kai Yuanqing Xiao, and Russ Tedrake. Evaluating robustness of neural networks with mixed integer programming. In *7th International Conference on Learning Representations*, 2019. 1
- [74] UN. The right to privacy in the digital age, 2021. 1, 3
- [75] Caterina Urban, Maria Christakis, Valentin Wüstholz, and Fuyuan Zhang. Perfectly parallel fairness certification of neural networks. *Proc. ACM Program. Lang.*, 2020. 3
- [76] Hanchen Wang, Nina Grgic-Hlaca, Preethi Lahoti, Krishna P. Gummadi, and Adrian Weller. An empirical study on learning fairness metrics for COMPAS data with human supervision. *CoRR*, 2019. 2
- [77] Tianlu Wang, Jieyu Zhao, Mark Yatskar, Kai-Wei Chang, and Vicente Ordonez. Balanced datasets are not enough: Estimating and mitigating gender bias in deep image representations. In *IEEE/CVF International Conference on Computer Vision*, 2019. 3
- [78] Zeyu Wang, Klint Qinami, Ioannis Christos Karakozis, Kyle Genova, Prem Nair, Kenji Hata, and Olga Russakovsky. Towards fairness in visual recognition: Effective strategies for bias mitigation. In *IEEE/CVF Conference on Computer Vision and Pattern Recognition*, 2020. 3
- [79] Benjamin Wilson, Judy Hoffman, and Jamie Morgenstern. Predictive inequity in object detection. *CoRR*, 2019. 3
- [80] Eric Wong and J. Zico Kolter. Learning perturbation sets for robust machine learning. In *ICLR*. OpenReview.net, 2021. 3
- [81] Samuel Yeom and Matt Fredrikson. Individual fairness revisited: Transferring techniques from adversarial robustness. In *Proceedings of the Twenty-Ninth International Joint Conference on Artificial Intelligence*, 2020. 1, 3
- [82] Mikhail Yurochkin, Amanda Bower, and Yuekai Sun. Training individually fair ML models with sensitive subspace robustness. In *8th International Conference on Learning Representations*, 2020. 1, 2
- [83] Mikhail Yurochkin and Yuekai Sun. Sensei: Sensitive set invariance for enforcing individual fairness. In *9th International Conference on Learning Representations*, 2021. 2
- [84] Richard S. Zemel, Yu Wu, Kevin Swersky, Toniann Pitassi, and Cynthia Dwork. Learning fair representations. In *Proceedings of the 30th International Conference on Machine Learning*, 2013. 1, 3
- [85] Han Zhao, Amanda Coston, Tameem Adel, and Geoffrey J. Gordon. Conditional learning of fair representations. In *8th International Conference on Learning Representations*, 2020. 3
- [86] Jieyu Zhao, Tianlu Wang, Mark Yatskar, Vicente Ordonez, and Kai-Wei Chang. Men also like shopping: Reducing gender bias amplification using corpus-level constraints. In *Proceedings of the 2017 Conference on Empirical Methods in Natural Language Processing*, 2017. 3

A. Proof of Theorem 4.1

This section provides a formal proof of the following:

Theorem 4.1. *Assume that we have a bijective generative model $G = D_G \circ E_G$ used to define the similarity set $S_i(\mathbf{x})$ for a given input \mathbf{x} . Let Alg. 1 perform center smoothing [45] with confidence $1 - \alpha_c$ and classification smoothing [11] with confidence $1 - \alpha_s$. If Alg. 1 returns CERTIFIED for the input \mathbf{x} , then the end-to-end model $M = \widehat{C} \circ \widehat{P} \circ E_G$ is individually fair for \mathbf{x} w.r.t. $S_i(\mathbf{x})$ with probability at least $1 - \alpha_c - \alpha_s$.*

Proof. Assume that Alg. 1 returns CERTIFIED for the input \mathbf{x} . We need to show that with high probability

$$\forall \mathbf{x}' \in S_i(\mathbf{x}). M(\mathbf{x}') = M(\mathbf{x}). \quad (7)$$

By definition of $S_i(\mathbf{x})$, it follows that for all $\mathbf{x}' \in S_i(\mathbf{x})$, there exists a $\mathbf{z}' \in S(\mathbf{x})$ such that $\mathbf{x}' = D_G(\mathbf{z}')$. By assumption, G is bijective, so $\mathbf{z}' = E_G(\mathbf{x}')$. That is, for all $\mathbf{x}' \in S_i(\mathbf{x})$, passing \mathbf{x}' through the first component of the model M (namely, E_G) results in a point $\mathbf{z}' \in S(\mathbf{x})$.

G and \mathbf{x} are given, so let us compute $\mathbf{z}_G = E_G(\mathbf{x})$. To prove the statement in Eq. (7), we now need to show that with high probability

$$\forall \mathbf{z}' \in S(\mathbf{x}). \left(\widehat{C} \circ \widehat{P} \right)(\mathbf{z}_G) = \left(\widehat{C} \circ \widehat{P} \right)(\mathbf{z}'). \quad (8)$$

The next step of the model pipeline computes $\widehat{P}(\mathbf{z})$ for a $\mathbf{z} \in \mathbb{R}^q$ in the latent space of the generative model G . \widehat{P} was defined such that $\widehat{P}(\mathbf{z}) = \widehat{g}_{\mathbf{z}}(0)$, where $\widehat{g}_{\mathbf{z}}(0)$ is the output of the center smoothed [45] function $g_{\mathbf{z}}(t) = P(\mathbf{z} + t \cdot \mathbf{a})$, $t \in \mathbb{R}$ at $t = 0$. Note that if $\mathbf{z}' = \mathbf{z} + t' \cdot \mathbf{a}$, then

$$\begin{aligned} g_{\mathbf{z}'}(t) &= P(\mathbf{z}' + t \cdot \mathbf{a}) \\ &= P(\mathbf{z} + t' \cdot \mathbf{a} + t \cdot \mathbf{a}) \\ &= P(\mathbf{z} + (t + t') \cdot \mathbf{a}) \\ &= g_{\mathbf{z}}(t + t') \end{aligned} \quad (9)$$

That is, $g_{\mathbf{z}'}(t) = g_{\mathbf{z}}(t + t')$, which implies $\widehat{g}_{\mathbf{z}'}(t) = \widehat{g}_{\mathbf{z}}(t + t')$, and in particular $\widehat{P}(\mathbf{z}') = \widehat{g}_{\mathbf{z}'}(0) = \widehat{g}_{\mathbf{z}}(t')$.

Now, let us get back to Eq. (8). For all $\mathbf{z}' \in S(\mathbf{x})$, by definition of $S(\mathbf{x})$, $\mathbf{z}' = \mathbf{z}_G + t' \cdot \mathbf{a}$ for some $t' \in [-\epsilon, \epsilon]$. Moreover, $\mathbf{z}_{cs} = \widehat{P}(\mathbf{z}_G) = \widehat{g}_{\mathbf{z}_G}(0)$ and $\widehat{P}(\mathbf{z}') = \widehat{g}_{\mathbf{z}_G}(t')$. Theorem 3.2 tells us that with probability at least $1 - \alpha_c$

$$\begin{aligned} \forall t' \in [-\epsilon, \epsilon]. \|\widehat{g}_{\mathbf{z}_G}(0) - \widehat{g}_{\mathbf{z}_G}(t')\|_2 &\leq r_{cs} \\ \iff \forall \mathbf{z}' \in S(\mathbf{x}). \|\mathbf{z}_{cs} - \widehat{P}(\mathbf{z}')\|_2 &\leq r_{cs}, \end{aligned} \quad (10)$$

provided that the center smoothing computation of \mathbf{z}_{cs} does not abstain.

Now, let us take a look at the final component of the pipeline – the smoothed classifier \widehat{C} . Provided that \widehat{C} does

not abstain at the input \mathbf{z}_{cs} , Theorem 3.1 provides us with a radius R around \mathbf{z}_{cs} such that with probability at least $1 - \alpha_s$

$$\begin{aligned} \forall \delta \text{ s.t. } \|\delta\|_2 < R, \widehat{C}(\mathbf{z}_{cs}) &= \widehat{C}(\mathbf{z}_{cs} + \delta) \\ \iff \forall \mathbf{z}'' \text{ s.t. } \|\mathbf{z}_{cs} - \mathbf{z}''\|_2 < R, \widehat{C}(\mathbf{z}_{cs}) &= \widehat{C}(\mathbf{z}''). \end{aligned} \quad (11)$$

If Alg. 1 returns CERTIFIED, that is $r_{cs} < R$, combining (10) and (11) and applying the union bound, we obtain that with probability at least $1 - \alpha_c - \alpha_s$ we have $\widehat{C}(\mathbf{z}_{cs}) = \widehat{C}(\widehat{P}(\mathbf{z}'))$ for all $\mathbf{z}' \in S(\mathbf{x})$. That is,

$$\forall \mathbf{z}' \in S(\mathbf{x}). \left(\widehat{C} \circ \widehat{P} \right)(\mathbf{z}_G) = \left(\widehat{C} \circ \widehat{P} \right)(\mathbf{z}'), \quad (12)$$

as required by (8). \square

B. Hyperparameter tuning

In this section, we perform an extensive hyperparameter search in order to select suitable values for the hyperparameters. We evaluate on 156 samples from the *validation* set of CelebA, on the *Smiling* task with a sensitive attribute *Pale_Skin*. Afterwards, we reuse the same hyperparameter values for all tasks with very minor changes. The hyperparameters which we tune, as well as the range of values that we consider about them, are as follows:

- $\lambda_1 \in \{0, 0.001, 0.0025, 0.005, 0.01, 0.025, 0.05, 0.1, 0.25, 0.5, 0.75\}$ – adversarial loss weight;
- $\lambda_2 \in \{0, 0.1, 0.25, 0.5\}$ – contrastive loss weight;
- $\delta \in \{10, 25, 50\}$ – contrastive loss radius;
- $\sigma_{enc} \in \{0.5, 0.75, 1\}$ – standard deviation of the Gaussian noise added during center smoothing;
- $\sigma_{cls} \in \{0.1, 0.25, 0.5, 1, 2.5, 5, 10, 25, 50\}$ – standard deviation of the Gaussian noise added during classifier smoothing.

Tuning σ_{enc} and the baselines We begin with selecting the value for σ_{enc} . It is not used during the training of L and C , but is an integral part of the center smoothing computation which is performed during inference and is the most time-consuming component of the model pipeline. More concretely, both $\mathbf{z}_{cs} = \widehat{P}(\mathbf{z}_G)$ and r_{cs} depend on σ_{enc} , in turn affecting both the accuracy and the certified individual fairness. We evaluate the Naive model with all candidate values for σ_{enc} and show the results in Tab. 6. We observe that there is little variation in terms of accuracy, while the best certified individual fairness is obtained at $\sigma_{enc} = 0.75$ and 1 . $\sigma_{enc} = 0.75$ produces a smaller average center smoothing radius, which is beneficial for certification

(see Alg. 1), therefore, we set $\sigma_{enc} = 0.75$ for all of the experiments (except for FairFace, where we use $\epsilon = 0.5$, therefore, we scale σ_{enc} correspondingly, *i.e.*, $\sigma_{enc} = 0.375$). Using the same σ_{enc} values for both LASSI and the baselines allows us to attribute the improvements of the results to the additional training mechanisms that we apply and not merely to different hyperparameter values.

We perform a similar evaluation on the validation set of the other baseline considered in this work, Data Augmentation, and from the results in Tables 6 and 7 we set $\sigma_{cls} = 10$ for Naive and $\sigma_{cls} = 5$ for Data Augmentation.

Tuning λ_1 Next, we incorporate the adversarial loss to the Naive training and explore the impact of λ_1 to the performance of the model in Tab. 8. We see that the certified individual fairness increases with increasing λ_1 . Moreover, for λ_1 from 0.001 to 0.5 the (non-trivial) accuracy corresponding to the highest certified individual fairness stays at approximately the same level. At $\lambda_1 = 0.75$ the model converges to making constant predictions, which achieves 100% certified individual fairness but is not very useful in terms of accuracy. We choose to proceed with $\lambda_1 = 0.1$, as it already gives most of the certified individual fairness boost which can be obtained using adversarial training, but also leaves more capacity to the model to potentially optimize the other loss terms.

Tuning LASSI: λ_2, δ and σ_{cls} We are now left with tuning the contrastive loss hyperparameters, as well as with selecting the σ_{cls} value for LASSI. Keeping $\lambda_1 = 0.1$, in Tab. 9 we evaluate all candidate pairs of λ_2 and δ on the CelebA validation set. We can see that LASSI outperforms the baselines and the Naive + Adversarial combination for a wide range of hyperparameters, concluding that it is not very sensitive to them. The certified individual fairness is slightly higher for $\lambda_2 = 0.1$ and for $\delta = 50$ in general. Therefore, we use these values as our default ones. Finally, most of the (λ_2, δ) pairs obtain their highest certified individual fairness with $\sigma_{cls} = 10$, so we run LASSI with $\sigma_{cls} = 10$ by default.

Is contrastive loss not enough? In the final step of our hyperparameter explorations, we verify that Naive combined only with contrastive loss is not enough. Indeed, this is confirmed by the results in Tab. 10, showing that this configuration performs worse than Naive + Adversarial and LASSI in terms of certified individual fairness. We provide a summary of our ablations in App. D.

C. More examples of similar individuals

Here, we provide further examples of points from the similarity sets $S_i(\mathbf{x})$, as reconstructed by Glow, for various

inputs \mathbf{x} randomly drawn from the test sets which we consider in our evaluation. A summary of all configurations is listed in Tab. 4. The images in the middle of the CelebA and FairFace reconstructions correspond to the original inputs. The perturbations range uniformly in the $[-\frac{\epsilon}{\sqrt{n}}, \frac{\epsilon}{\sqrt{n}}]$ interval, where n is the number of sensitive attributes. For $n > 1$, all attribute vectors are multiplied by the same t before they are added to the latent representation of the original inputs. We set $\epsilon = 1$ for CelebA and 3D Shapes and $\epsilon = 0.5$ for FairFace.

Dataset	Sensitive attribute(s)	Figure
CelebA	Pale_Skin	Figure 6
	Young	Figure 7
	Blond_Hair	Figure 8
	Heavy_Makeup	Figure 9
	Pale + Young	Figure 10
FairFace	Pale + Young + Blond	Figure 11
	Race=Black	Figure 12
3D Shapes	orientation	Figure 13

Table 4. Summary of the provided example images from the similarity sets considered in this work.

D. Ablation study

Table 5 summarizes the best results obtained by Naive, Naive + Adversarial and Naive + Contrastive on the validation subset of CelebA for the Smiling task with a sensitive attribute Pale_Skin. For LASSI we use the same configuration that was used to produce the results in the main paper (where we evaluate on the test set). The results confirm our hypothesis that both the adversarial and contrastive losses help to increase the certified individual fairness but combining them improves the results further.

Method	Acc. (%)	Fair (%)
Naive	91.03	7.05
Naive + Adversarial ($\lambda_1 = 0.5$)	90.38	60.26
Naive + Contrastive ($\lambda_2 = 0.5, \delta = 50$)	92.95	49.36
LASSI ($\lambda_1 = \lambda_2 = 0.1, \delta = 50$)	89.10	70.51

Table 5. Ablation study of our method, performed on the CelebA validation subset for the task Smiling with a sensitive attribute Pale_Skin.

σ_{enc}	Mean r_{cs}	Metric	σ_{cls}								
			0.1	0.25	0.5	1	2.5	5	10	25	50
0.5	50.96	Acc. (%)	92.95	92.31	92.31	92.31	92.31	91.03	91.67	90.38	80.13
		Fair (%)	0	0	0	0	0	4.49	4.49	0.64	0
0.75	41.57	Acc. (%)	92.31	92.31	91.67	92.31	91.67	91.67	91.03	90.38	80.77
		Fair (%)	0	0	0	0	3.21	6.41	7.05	3.21	0
1	42.99	Acc. (%)	91.67	91.67	91.67	91.67	91.03	91.03	91.67	90.38	82.05
		Fair (%)	0	0	0	0	2.56	7.05	7.05	3.21	0

Table 6. Results of Naive on the validation subset of CelebA for different values of σ_{enc} and σ_{cls} . The second column contains the mean center smoothing radii corresponding to the different σ_{enc} values. Smaller is generally better for certified individual fairness (see the condition in Alg. 1).

σ_{enc}	Mean r_{cs}	Metric	σ_{cls}								
			0.1	0.25	0.5	1	2.5	5	10	25	50
0.75	18.93	Acc. (%)	92.31	91.67	91.67	92.31	92.95	92.95	91.03	86.54	66.67
		Fair (%)	0	0	0	4.49	13.46	23.08	22.44	8.97	3.21

Table 7. Results of the Data Augmentation baseline on the validation set of CelebA for $\sigma_{enc} = 0.75$ and different values of σ_{cls} .

λ_1	Metric	σ_{cls}								
		0.1	0.25	0.5	1	2.5	5	10	25	50
0.001	Acc. (%)	91.67	91.67	91.67	91.03	90.38	91.03	90.38	85.26	47.44
	Fair (%)	0	0	0	0	12.82	13.46	11.54	1.28	0
0.0025	Acc. (%)	91.03	91.03	90.38	90.38	90.38	89.74	89.74	77.56	48.72
	Fair (%)	0	0	0	8.33	21.15	19.87	14.74	1.92	2.56
0.005	Acc. (%)	91.03	91.03	91.03	91.67	90.38	91.67	92.31	66.03	48.72
	Fair (%)	0	0	3.85	16.03	26.92	25.64	16.03	6.41	7.05
0.01	Acc. (%)	92.31	92.31	92.31	92.31	92.95	92.95	88.46	48.72	48.08
	Fair (%)	0	0.64	12.18	28.85	30.77	28.21	16.03	8.33	16.03
0.025	Acc. (%)	92.95	92.95	92.31	92.31	91.03	90.38	81.41	48.08	46.15
	Fair (%)	0.64	8.97	30.13	43.59	42.31	35.90	21.79	21.79	36.54
0.05	Acc. (%)	91.03	91.03	91.03	90.38	91.03	90.38	51.92	49.36	48.72
	Fair (%)	1.28	23.72	46.15	48.72	48.72	39.10	24.36	41.03	59.62
0.1	Acc. (%)	90.38	90.38	90.38	89.10	87.18	86.54	49.36	48.72	47.44
	Fair (%)	8.97	36.54	53.21	58.97	53.85	46.15	31.41	50.64	69.23
0.25	Acc. (%)	91.67	89.74	89.10	89.74	89.74	53.21	50.00	49.36	48.08
	Fair (%)	28.21	54.49	57.69	57.69	50.64	32.69	55.13	72.44	82.69
0.5	Acc. (%)	89.74	89.74	90.38	89.74	87.18	50.64	49.36	48.72	48.08
	Fair (%)	30.13	58.97	60.26	60.26	50.64	34.62	60.26	76.92	89.10
0.75	Acc. (%)	50	50	50	50	50	50	50	48.08	48.08
	Fair (%)	98.08	100	100	100	100	100	100	98.08	96.79

Table 8. Results of Naive + Adversarial on the validation subset of CelebA for different values of λ_1 and σ_{cls} , while keeping $\sigma_{enc} = 0.75$. Certified individual fairness increases with increasing λ_1 .

λ_2	δ	Mean r_{cs}	Metric	σ_{cls}									
				0.1	0.25	0.5	1	2.5	5	10	25	50	
0.1	10	19.02	Acc. (%)	91.03	91.03	90.38	89.74	89.10	89.10	89.10	87.18	48.08	
			Fair (%)	0	2.56	22.44	53.21	69.87	71.79	71.79	62.18	30.77	
	25	11.88	Acc. (%)	91.03	91.67	91.67	90.38	89.74	89.74	89.74	89.10	89.10	
			Fair (%)	1.92	23.72	48.08	62.82	68.59	73.08	76.28	75.00	71.79	
	50	10.49	Acc. (%)	89.74	89.74	91.03	89.74	89.74	89.10	89.10	89.10	89.10	
			Fair (%)	2.56	24.36	43.59	54.49	64.74	69.23	70.51	70.51	67.95	
0.25	10	13.55	Acc. (%)	89.10	89.10	89.74	89.10	89.10	89.10	89.10	89.10	46.79	
			Fair (%)	0	0	1.92	19.23	57.69	60.26	59.62	30.13	12.82	
	25	16.83	Acc. (%)	90.38	89.74	90.38	89.74	88.46	89.10	89.74	88.46	86.54	
			Fair (%)	0	28.21	47.44	59.62	65.38	66.03	67.31	67.31	65.38	
	50	11.95	Acc. (%)	89.74	89.74	89.1	89.1	88.46	88.46	88.46	87.82	87.82	
			Fair (%)	0.64	23.72	47.44	60.26	69.87	70.51	72.44	72.44	70.51	
0.5	10	15.1	Acc. (%)	91.03	91.03	91.03	91.03	91.03	91.03	91.03	91.03	47.44	
			Fair (%)	0	0	0	14.74	56.41	61.54	57.05	25.00	11.54	
	25	21.35	Acc. (%)	90.38	90.38	90.38	90.38	91.67	91.67	91.03	91.03	89.74	
			Fair (%)	0	6.41	37.18	55.77	62.18	64.10	65.38	64.74	62.18	
	50	16.87	Acc. (%)	91.03	91.03	91.03	89.74	89.74	89.74	89.74	89.74	89.1	
			Fair (%)	0	3.85	31.41	50.00	66.67	71.15	75.00	73.72	66.67	

Table 9. Results of LASSI on the validation subset of CelebA for different values of λ_2 , δ and σ_{cls} , while keeping $\sigma_{enc} = 0.75$ and $\lambda_1 = 0.1$. LASSI works well, outperforming the baselines, for a wide range of hyperparameters.

λ_2	δ	Metric	σ_{cls}								
			0.1	0.25	0.5	1	2.5	5	10	25	50
0.1	10	Acc. (%)	90.38	90.38	90.38	90.38	90.38	90.38	90.38	90.38	90.38
		Fair (%)	0	0	0	0	16.03	37.18	46.79	41.03	25.64
	25	Acc. (%)	91.67	91.67	91.03	90.38	90.38	90.38	90.38	90.38	91.03
		Fair (%)	0	0	0.64	9.62	35.90	45.51	46.79	46.15	38.46
	50	Acc. (%)	91.03	91.03	91.67	92.31	92.31	92.31	92.31	91.67	91.67
		Fair (%)	0	0	0	5.77	35.9	42.95	47.44	43.59	39.1
0.25	10	Acc. (%)	92.31	92.31	92.31	92.31	92.31	92.31	92.31	92.31	92.31
		Fair (%)	0	0	0	0	17.95	35.90	44.87	41.67	19.87
	25	Acc. (%)	92.95	92.95	92.95	92.31	91.67	91.67	92.95	92.95	92.95
		Fair (%)	0	0	1.28	11.54	35.9	42.95	48.72	46.79	39.74
	50	Acc. (%)	92.95	92.31	92.31	91.67	91.67	91.67	91.67	91.67	91.67
		Fair (%)	0	0	2.56	17.31	33.33	45.51	48.72	48.72	37.18
	10	Acc. (%)	91.03	90.38	91.03	91.03	91.03	91.03	91.03	91.03	48.72
		Fair (%)	0	0	0	0	0	0.64	0	0	0
	25	Acc. (%)	89.74	89.74	89.74	89.1	89.1	89.1	89.1	89.74	90.38
		Fair (%)	0	0	0.64	7.69	35.26	44.23	48.08	46.79	38.46
	50	Acc. (%)	92.95	92.95	92.31	92.95	92.95	92.95	92.95	92.95	92.31
		Fair (%)	0	0	7.05	20.51	36.54	45.51	49.36	48.72	40.38

Table 10. Results of Naive + Contrastive on the validation subset of CelebA for different values of λ_2 , δ and σ_{cls} , while keeping $\sigma_{enc} = 0.75$ and $\lambda_1 = 0$. Contrastive loss only is not enough to obtain the same improvements in certified individual fairness, compared to Naive + Adversarial and LASSI.

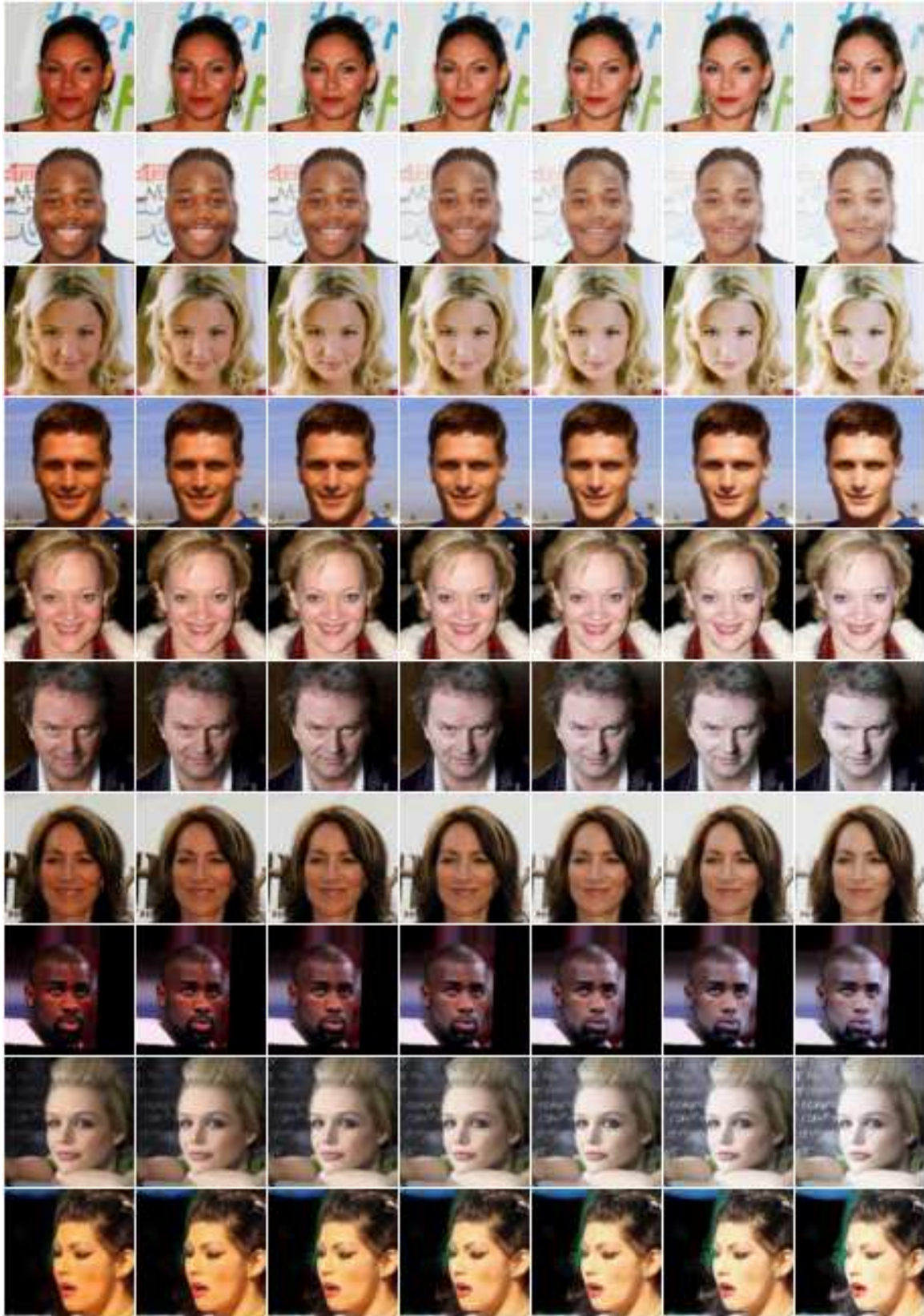


Figure 6. Similar individuals from $S_i(\mathbf{x})$, for \mathbf{x} in the CelebA dataset, obtained by varying the sensitive attribute Pale_Skin.

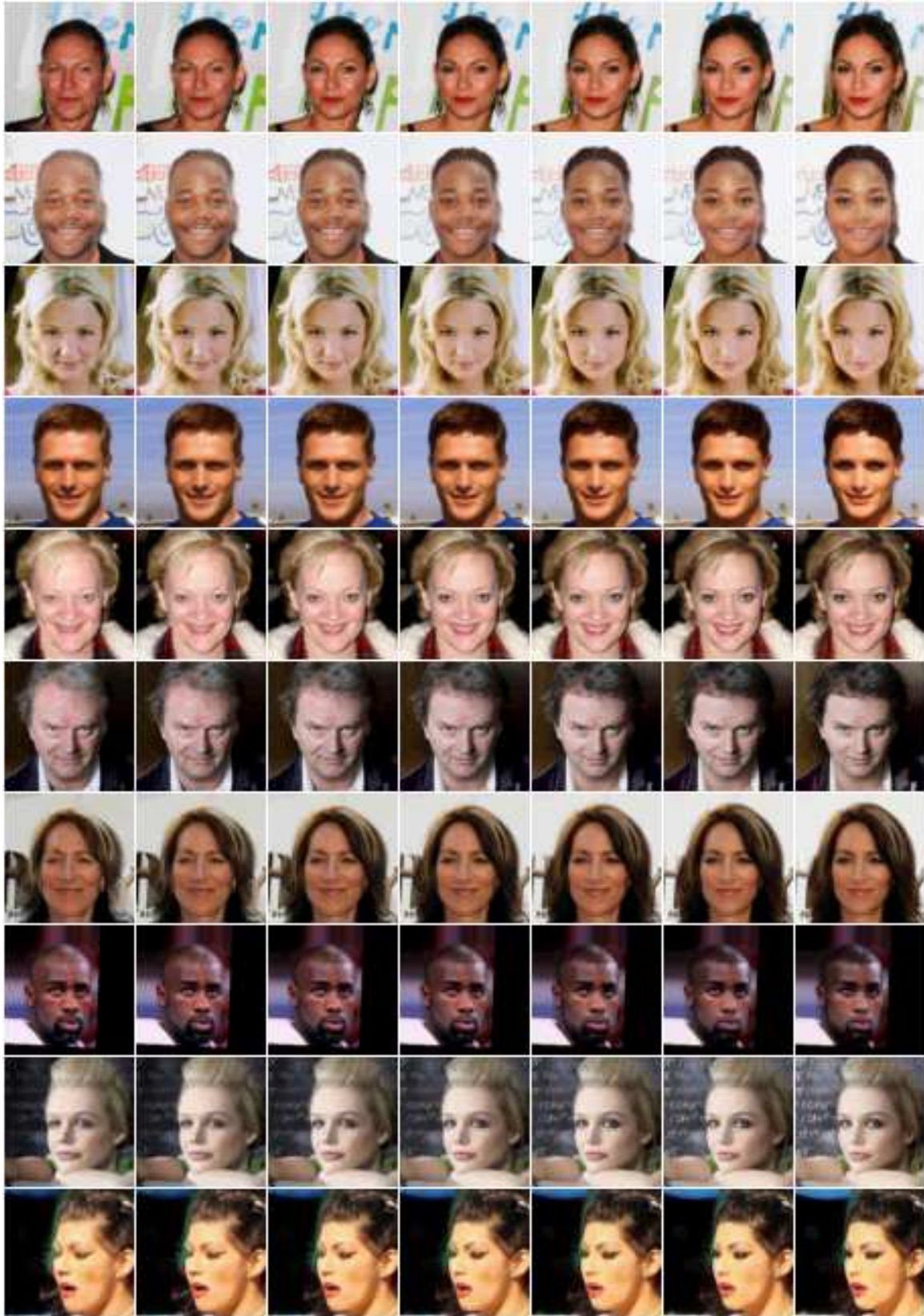


Figure 7. Similar individuals from $S_i(\mathbf{x})$, for \mathbf{x} in the CelebA dataset, obtained by varying the sensitive attribute Young.



Figure 8. Similar individuals from $S_i(\mathbf{x})$, for \mathbf{x} in the CelebA dataset, obtained by varying the sensitive attribute `Blond_Hair`.

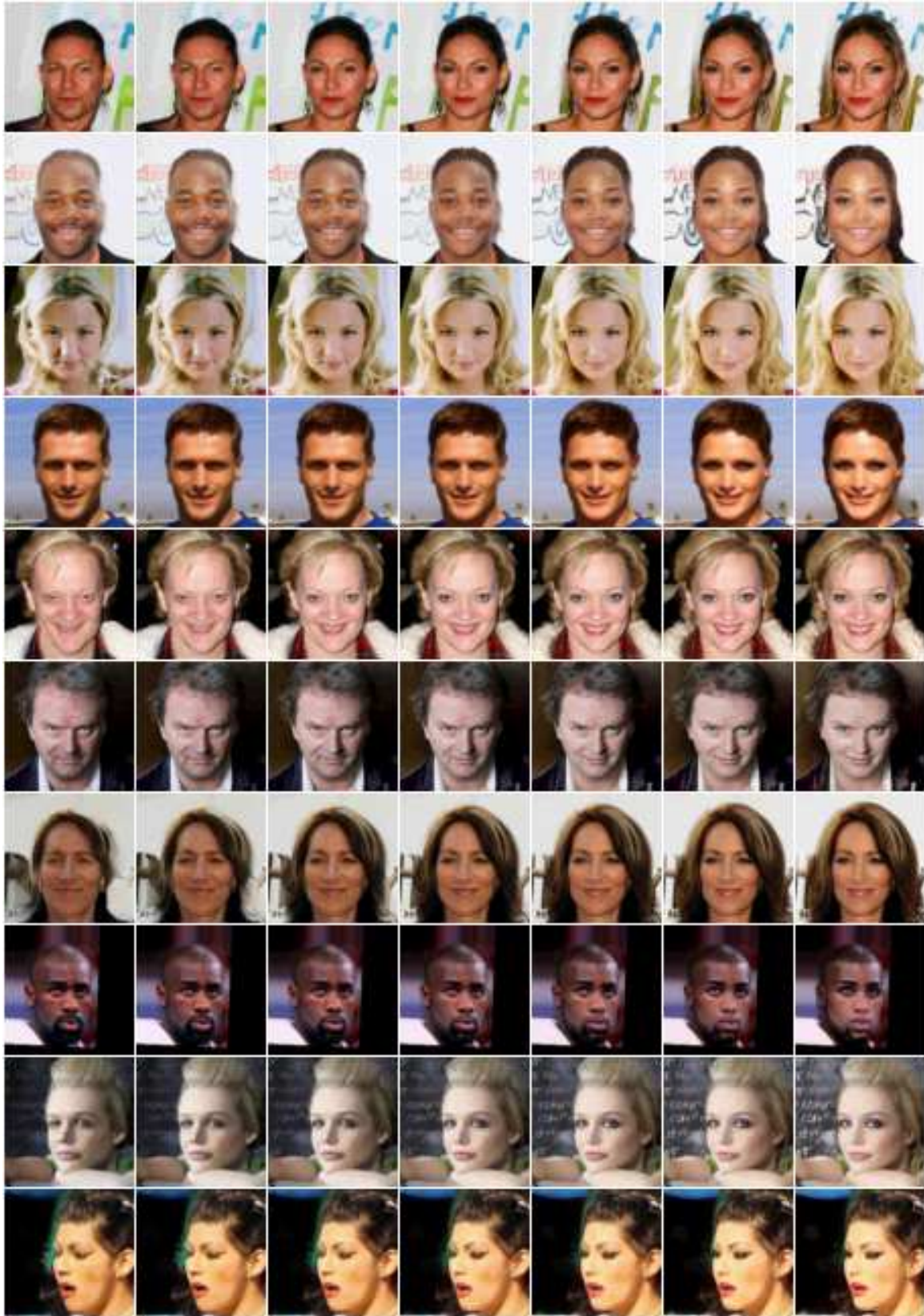


Figure 9. Similar individuals from $S_i(\mathbf{x})$, for \mathbf{x} in the CelebA dataset, obtained by varying the sensitive attribute Heavy_Makeup.

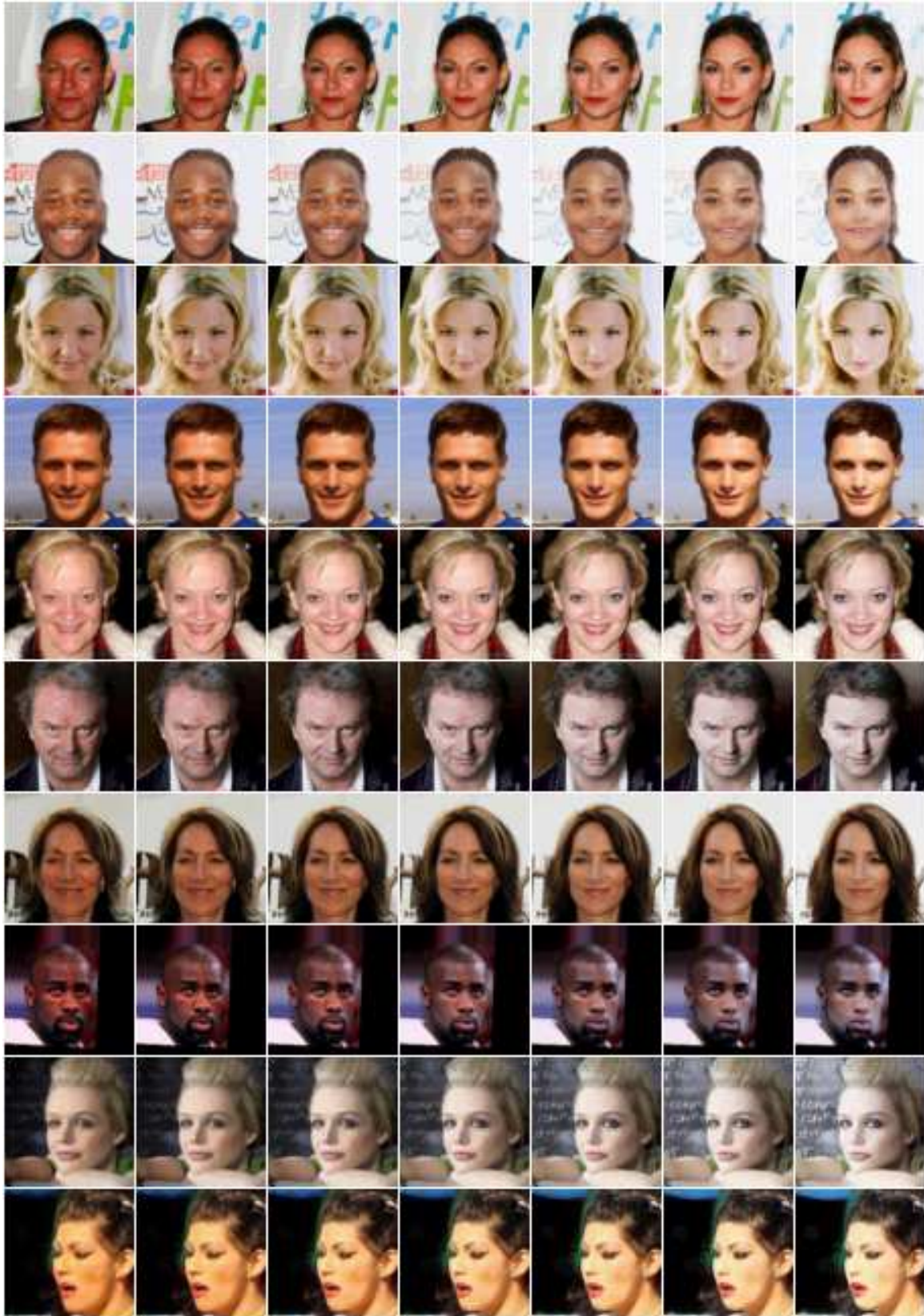


Figure 10. Similar individuals from $S_i(\mathbf{x})$ obtained by simultaneously varying the sensitive attributes Pale_Skin + Young.

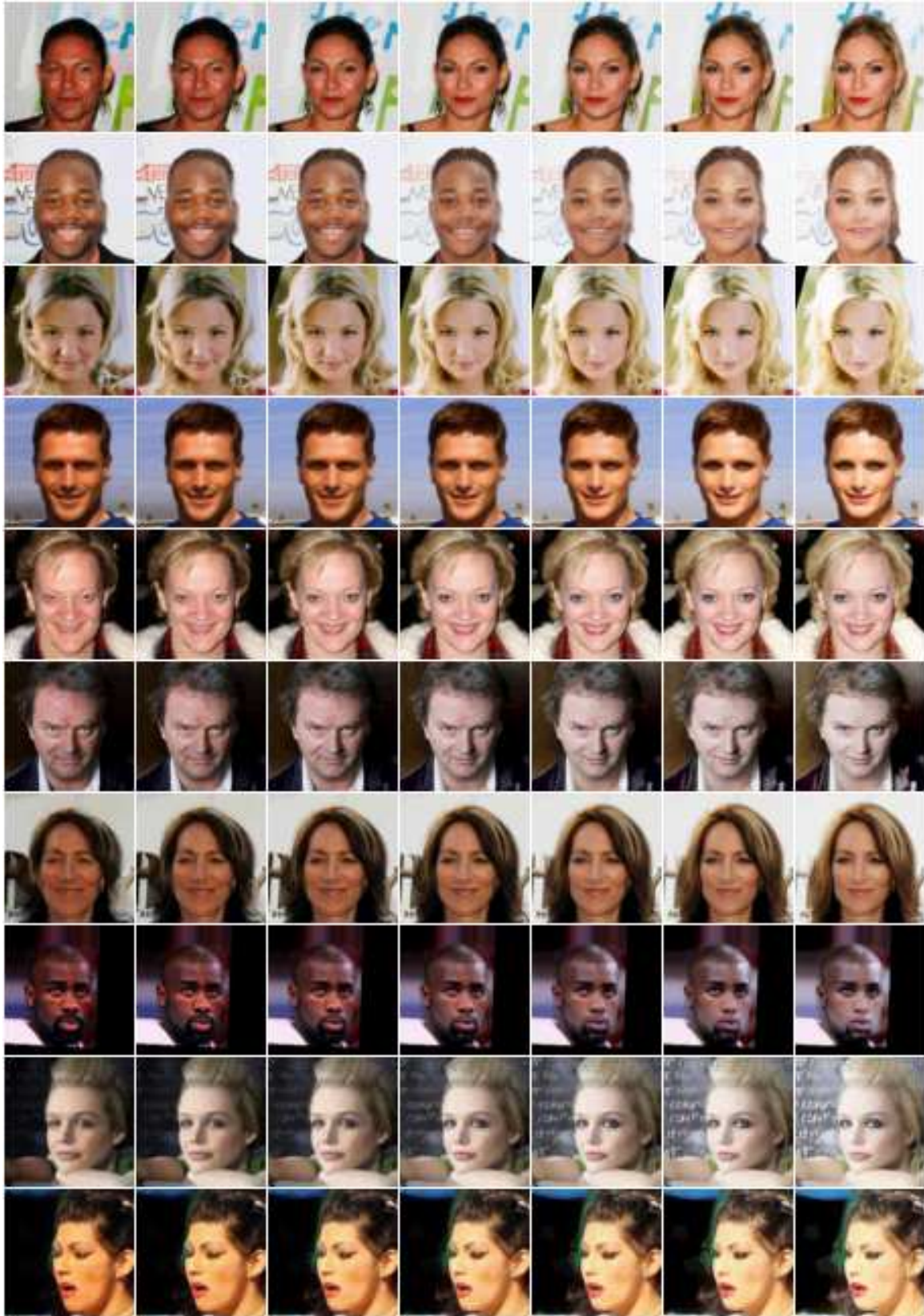


Figure 11. Similar individuals from $S_i(\mathbf{x})$ obtained by simultaneously varying the sensitive attributes Pale_Skin + Young + Blond.



Figure 12. Similar individuals from $S_i(\mathbf{x})$, for \mathbf{x} in FairFace and $\epsilon = 0.5$, obtained by varying the sensitive attribute Race=Black.

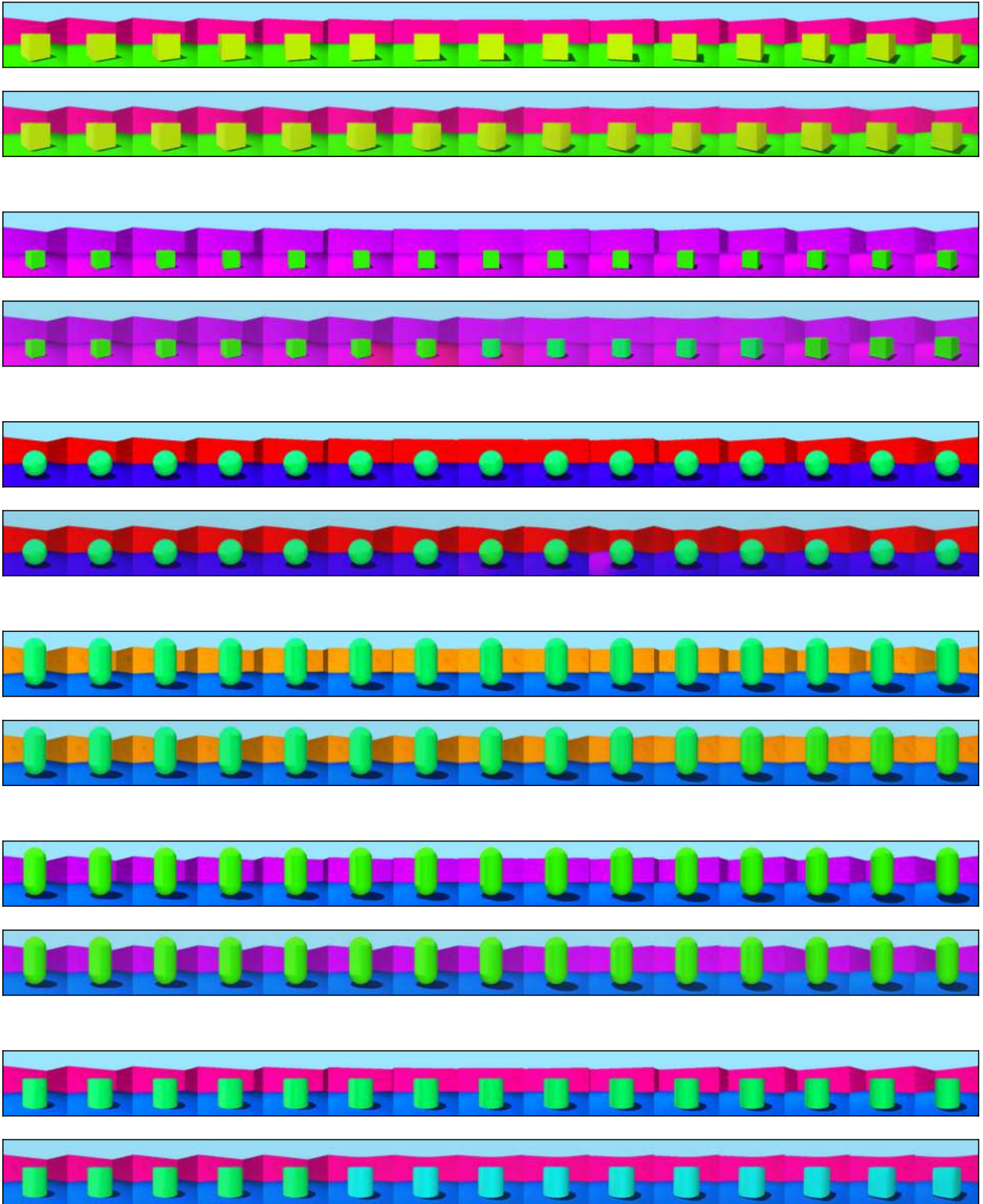


Figure 13. Sampled shapes at 15 different ground truth orientations. The original (above) and the corresponding reconstructions (below) obtained from interpolating along the generative model's attribute vector are grouped together.